Spring 5-2013

Investigation of Adhesion and Network Properties In Thiol-Ene Polymer Networks Modified With Catechol Functionality For Improved Stone Conservation

Ethan F.T. Hoff
University of Southern Mississippi

The University of Southern Mississippi

INVESTIGATION OF ADHESION AND NETWORK PROPERTIES IN THIOL-ENE POLYMER NETWORKS MODIFIED WITH CATECHOL FUNCTIONALITY FOR IMPROVED STONE CONSERVATION

By

Ethan F. T. Hoff

A Thesis

Submitted to the Honors College of
The University of Southern Mississippi
In Partial Fulfillment
of the Requirements for the Degree of
Bachelor of Science
in the Department of Polymer Science and High Performance Materials

April 2013

Approved by

_____

Derek L. Patton
Professor of Polymer Science

_____

Robert Y. Lochhead, Director
Department of Polymers and
High Performance Materials

_____

David R. Davies, Dean
Honors College

Table of Contents:

ACKNOWLEDGMENTS……v

LIST OF ABBREVIATIONS AND KEY TERMS……..vi

ABSTRACT …….vii

CHAPTER I: INTRODUCTION ……...……...1

CHAPTER II: LITERATURE .……..5

CHAPTER III: EXPERIMENTAL METHODS…..……..8

1.1 Materials ……..….8

1.2 Synthesis……...9

1.3 Film Preparation……..……11

1.4 Characterization……..…12

CHAPTER IV: RESULTS ……...14

CHAPTER V: CONCLUSIONS ….…….……25

REFERENCES ……...……..26

ACKNOWLEDGMENTS

I would like to give my wholehearted thanks to my research advisor, Dr. Derek Patton, for guiding me over the last two years. My time spent conducting research in the Patton research group has left me with invaluable experience and skills that will benefit me throughout my career. Dr. Patton has always been very generous with both his time and his expertise in the area of crosslinked thiol-ene networks. I would like to extend a special thanks to Bradley Sparks who I worked under in the Patton research group for the countless hours of mentoring and all the things that I have learned lab. I would also like to thank Dr. Robert Lochhead for the time I spent in his research group. Dr. Lochhead never missed an opportunity to inspire me to become a creative and innovative scientist as well as encouraging me to take the initiative in my research endeavors. I was also fortunate enough to work for Dr. Jeffery Wiggins and I am very thankful for the introduction I received to the academic research community while working in his research group.

My parents, Fred and Tara Hoff, have supported me with a never-ending love and encouragement and have always propelled me to be the absolute best version of myself. My older sisters, Emily and Olivia, they have always been shining examples in academics, research, and life. My sisters have provided me with help whenever I needed them without fail throughout my education and I would not be where I am without them.

I would like to acknowledge the National Science Foundation, the Office of Naval Research, and the Alliance for Graduate Education in Mississippi Summer Research Experience for Undergraduates for funding and support of this project.

LIST OF ABBREVIATIONS

APE	Penaerythritol Triallyl Ether
PETMP	Pentaerythritol tris(3-mercaptopropionate)
DAm	Dopamine Acrylamide
RT-FTIR	Real-Time Fourier Transform Infrared Spectroscopy
DSC	Differential Scanning Calorimetry
DMA	Dynamic Mechanical Analysis
T_g	Glass Transition Temperature
DMPA	2,2-dimethoxy-2-phenyylacetophenone
PhEAm	Phenethyl Acrylamide

ABSTRACT

In this thesis, thiol-ene networks of pentaerythritol allyl ether (APE) and pentaerythritol tris(3-mercaptopropionate) (PETMP) modified with dopamine acrylamide (DAm) containing catechol functionality were formulated and tested in order to investigate the effect the catechol group has on major network properties and adhesion. DAm-APE-PETMP networks were successfully synthesized and applied to a wide variety of substrates (Glass, Steel, Aluminum, etc.) in order to test adhesion. The networks were also characterized using infrared spectroscopy, photo-dynamic scanning calorimetry, dynamic mechanical analysis, and tensile testing. Improved macroscopic adhesion values over the neat APE-PETMP networks were achieved on a variety of substrates including steel, aluminum, stone, and glass. Increases in glass transition temperature (T_g), glassy storage modulus, and toughness were observed with increasing concentration of DAm. Crosslink density and storage modulus above T_g decreased with increasing concentration of DAm.

CHAPTER I:

INTRODUCTION

Human society has been crafting stone into shelters, artworks, or objects of worship for millennia. Much of society's cultural heritage has been immortalized in stone because it is considered to be a very durable material. Stone plays a large and varied role in our culture being used for anything from a gravestone to a skyscraper. Although stone is an incredibly long-lasting material, it is subject to a variety of agents that cause deterioration and weathering (Winkler, 1994; Amoroso, 1983). These agents include cycles of hot and cold temperature extremes, wet and dry conditions, ultraviolet radiation exposure, both acids and bases, as well as, pollutant chemicals that can attack and degrade the stone. Carbonaceous stones such as limestone and marble are especially susceptible to degradation by "acid rain" or dry deposition of sulfur dioxide (Charola, 1998). There are a variety of materials currently used in the field to treat deteriorating stone. In general, stone treatments fall within one of four categories: cleaning, desalination, consolidation, and water repellents. In some cases adhesives are used to make repairs to stone materials (Price, 1996). Cultural heritage items, however, possess unique treatment requirements which make finding and implementing appropriate treatments difficult.

This project seeks to develop modified thiol-X (where X is an –ene such as (meth)acrylates, vinyl ethers, etc.) polymers that can be applied as a liquid resin to the porous surface of stone and subsequently photopolymerized using ultraviolet radiation to form a protective coating while maintaining the general aesthetics of the stone. Thiol-ene photopolymerization has been proposed as a possible method for improvement over those

materials used in stone consolidation instead of thermally initiated polymerization due to the more easily met requirements for initiation (Nason, 2005). These systems may provide a method of consolidation by means of infusing liquid resin precursors into stone and subsequently initiating polymerization by exposing the stone/polymer interface to light. The thiol-ene approach has numerous advantages over current (meth)acrylate systems. One such advantage is that the glass transition temperature (T_g) can be tuned with ease (i.e. -10 to 90 ^oC) by carefully choosing the thiol and "ene" components from commercially available compounds. Another advantage of thiol-ene networks is their formation through a stepwise manner facilitated by a very rapid and highly efficient free-radical chain transfer reaction shown in Figure 1, also these reactions only reach a gel point at relatively high functional group conversion (Charles, 2010).

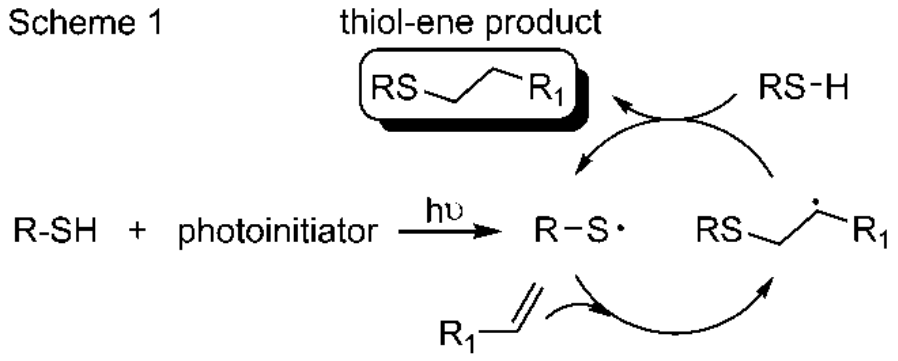

Figure 1. Thiol-ene free-radical chain transfer reaction.

Furthermore, through the chain transfer process with thiols, oxygen inhibition sensitivity typically observed in (meth)acrylate systems, is significantly reduced which is important because an inert atmosphere will not be present in the treatment of all stone surfaces (O'Brien, 2006). The last advantage to discuss is the fact that thiol-ene resins in

the pre-cured state are often liquids which is beneficial when applying to a porous surface like stone because it allows the resin to penetrate deeper into the stone. In addition, the liquid resins can often be cured in the absence of volatile organic solvents which reduces environmental impact. Stone treatment consists of multiple complex factors to be considered such as the stone composition and structure, the nature of the polymer treatment, the stone-treatment interaction, and the long term effects on the stone-treatment matrix. The interface between stone (or model surfaces) and the thiol-ene polymer consolidants will be studied using a variety of techniques including microscopy, spectroscopy, nanoindentation, and scattering techniques. Using a combination of flexural strength and microabrasion tests the mechanical properties of the consolidant treated stone will be tested. Long term performance of the stone consolidants will be characterized using artificial weathering techniques and field studies. These tests will be performed with the ultimate goal being the development of an advanced approach to stone conservation based on thiol-ene polymer systems designed to improve stone consolidation. The focus of this project is the development of new treatments for stone consolidants and water repellents, more specifically the effects of a variety of functionalities on adhesion and other network properties. One such moiety is the catechol functionality found in dopamine acrylamide (DAm). For example, DAm will be incorporated into the thiol-X network via the acrylamide group and compared to an identical chemical structure without the 3,4-dihydroxy functionality of the catechol, phenethyl acrylamide (PhEtAm), in order to further elucidate the role of the catechol on network properties. DAm is a derivative of the 3,4-dihydroxyphenylalanine (DOPA) which plays a major role in the natural adhesive capabilities of intertidal marine species

such as mussels and polychaetes (Stewart, 2004). A schematic version of the network is shown below in Figure 2.

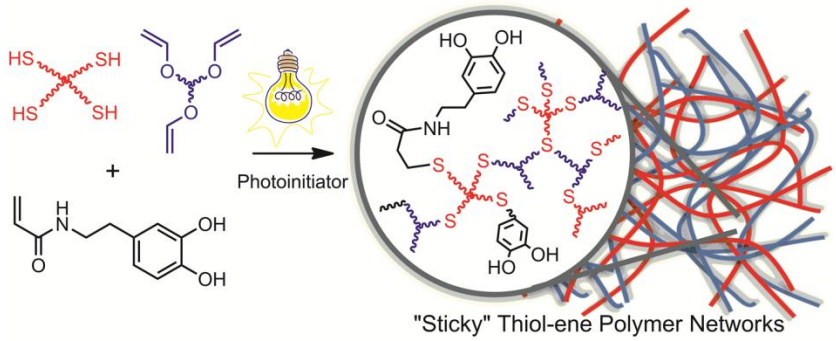

Figure 2. Synthetic route to catechol functionalized thiol-ene polymer networks by photopolymerization

DOPA derivatives have been incorporated into many types of systems where exhibit improved adhesive and cohesive properties in a variety of applications and on various substrates. The types of stone targeted include Salem Indiana limestone, Royal Danby Vermont marble, and Connecticut Portland Brownstone sandstone.

CHAPTER II:

LITERATURE REVIEW

Stone in Architecture written by Dr. E. M. Winkler in 1994 provides a survey of key properties of stone, both physical and chemical, pertaining to architecture, engineering, and stone production. Winkler et al. emphasize the chemical characteristics of air and water-borne pollutants which can accelerate the stone decay process. All of these factors being fundamental to stone conservation efforts make this book valuable to better understand the nature of stone decay and therefore stone conservation (Winkler, 1994).

In 1983 Giovanni Amoroso and Vasco Fassina published *Stone Decay and Conservation.* Amoroso and Fassina compiled a large number of references to scientific and scholarly works on the decay and conservation of stone while also detailing many phenomena and deterioration mechanisms through scientific examination. This book has served to bring up many stone decay mechanisms which might not have been thought of otherwise (Amoroso, 1983).

The *Review of Literature on the Topic of Acidic Deposition on Stone* written for the National Center for Preservation Technology and Training by A. Elena Charola is a survey focused on presenting a summary of the relevant publications related to the field of acid precipitation which is one of the leading causes of decay in stone. This review provided information fundamental to understanding the causes and relative severity of these sources of weathering (Charola, 1998).

Stone Conservation: An Overview of Current Research written by Clifford Price is a highly comprehensive book on the subject of stone conservation. This book details

many of the facets of stone conservation, including, but not limited to characterization of stone, causes of decay, prevention and treatment of decay, along with assessments of these treatments and the authors thoughts on the future of stone conservation. Price's work has proven to be invaluable in the understanding of stone decay and the treatment methods already being pursued (Price, 1996).

Nason and colleagues in their journal article "UV-induced Frontal Polymerization of Multifunctional (Meth)acrylates" propose a system that can be polymerized via ultraviolet irradiation to initiate a frontal polymerization. Although the techniques used in the execution of this thesis are not frontal polymerizations the theories behind the UV initiated system and its application in stone conservation and consolidation are both important to the experiment at large (Nason, 2005).

Thiol-ene click reactions exhibit all the characteristics which Sharpless used to categorize idealized reactions such as high selectivity, simple orthogonal reactions that do not yield side products, and give heteroatom-linked molecular systems with high efficiency under a variety of mild conditions. In the case of thiol-ene reactions, they are frequently photoinitiated polymerizations that typically result in highly uniform networks that promote unique capabilities and opportunities for control. In the article "Thiol-Ene Click Chemistry", Hoyle and colleagues review these reactions focused on the reaction mechanism, the varied methodologies, functionalization, surface and polymer modification, and polymerization (Charles, 2010).

Due to the typical open-air nature of stone consolidation applications, it is important to take into account the effect oxygen may have on the polymerization process. Work done by O'Brien and colleagues in "Oxygen Inhibition in Thiol-Acrylate

Photopolymerizations" showed that propionate thiol monomers were more reactive and polymerized to a greater extent when oxygen was present than other monomer choices. These findings had a great deal of impact on the monomer choice for the system that will be used in this thesis (O'Brien, 2006).

The marine polychaete, *Phragmatopoma californica*, builds protective tubes using bits of shell and sand joined by secreted proteinaceous cement forming a foam substance which is then solidified by the oxidative coupling of DOPA molecules. This process has inspired the use of DOPA and DOPA derivatives in the pursuit of enhanced adhesive properties in a wide range of applications. "The Tube Cement of *Phragmatopoma californica*: A Solid Foam" written by Stewart and colleagues examines the structure and chemical makeup of this cement in great detail (Stewart, 2004).

The synthetic procedures for the monomers acrylic anhydride, phenethyl acrylamide, and dopamine acrylamide (DAm) were used directly or adapted from articles by Hammaker, Frost, and Chung, respectively (Hammaker, 2008; Frost, 2008; Chung, 2011).

CHAPTER III:

EXPERIMENTAL METHODS

1.1 *Materials*

All reagents and solvents used throughout these experiments were obtained at the highest purity available from Aldrich Chemical Company and used without further purification unless otherwise specified. Acrylic acid, acryloyl chloride, N,N-diisobutylethylamine (DIEA), sodium tetraborate decahydrate, 3,4-dihydroxyphenethylamine hydrochloride, 2,2-dimethoxy-2-phenyylacetophenone (DMPA), and pentaerythritol triallyl ether (APE) were obtained from Sigma-Aldrich, sodium bicarbonate and magnesium sulfate were obtained from Fisher Scientific, and pentaerythritol tetra(3-mercaptopropionate) (PETMP) was obtained from Bruno Bock. Acrylic anhydride, phenethyl acrylamide, and dopamine acrylamide (DAm) were synthesized using procedures found in literature.

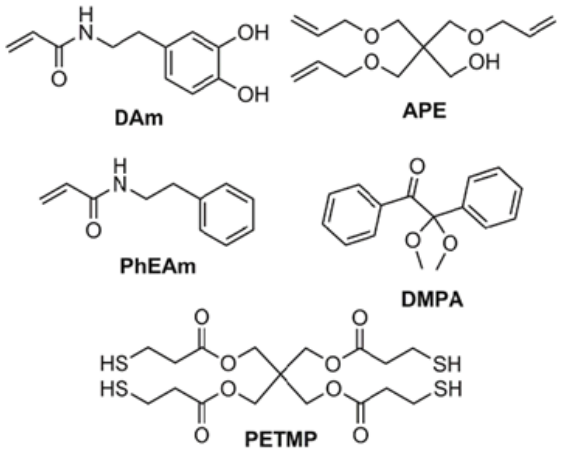

Figure 3. Chemical structures of monomers and photoinitiator.

1.2 *Synthesis*

Acrylic anhydride was synthesized according to a previously reported procedure. Diethyl ether (30 mL) and acrylic acid (3 mL, 0.044 mol) were added to a round bottom flask and purged with N_2 gas while stirring. N,N-diisobutylethylamine (DIEA) (7.62 mL, 0.044 mol) was slowly added to the stirring solution via syringe. Acryloyl chloride (3.74 mL, 0.046 mol) was added dropwise to the solution using a syringe pump. A precipitate was formed and the reaction mixture was stirred for 30 min. The precipitate was removed using vacuum filtration and subsequently washed with diethyl ether. The filtrate and washings were combined and concentrated using a rotary evaporator to yield and orange oil. The product was distilled using a Vigreaux column, yielding a colorless oil. ^{1}H and ^{13}C NMR spectra correspond with those which were reported in literature (Hammaker, 2008).

Phenethyl acrylamide (PhEtAm) was synthesized according to a previously reported procedure. A solution of phenethylamine (2.42 g, 0.020 mol) and dichloromethane (25 mL) was added to a round bottom flask and subsequently cooled to 0 ^{o}C. Triethylamine (2.12 g, 0.021 mol) was added to the solution followed by the drop-wise addition of acrylic anhydride (1.90 g, 0.020 mol) in dichloromethane (5 mL). The solution stirred at 4 ^{o}C for 3 hours. The solution was brought to room temperature before being quenched using 1 M HCl (30 mL). The organic layer was washed using 1 M NaOH (30 mL), saturated NaCl (30 mL), and dried over $MgSO_4$. The resulting solution was concentrated using a rotary evaporator. The solution was passed through a silica pad using 6:1 solution of hexanes:ethyl acetate to remove any side products. The product was

dried under vacuum and the molecular structure was confirmed using proton and carbon NMR (Frost, 2008).

DAm was synthesized from a modified literature procedure. In a round bottom flask, sodium borate (10 g, 0.026 mol) and sodium bicarbonate (4 g, 0.048 mol) were added to 100 mL of deionized water. The aqueous solution was degassed by bubbling nitrogen through the solution for 20 min. Following the degassing, 3,4-dihydroxyphenethylamine hydrochloride (5 g, 0.026 mol) was added to the stirring solution. In a separate flask, acrylic anhydride (4.7 mL) was diluted in 20 mL of tetrahydrofuran (THF). This solution was added drop-wise to the round bottom flask containing the aqueous reaction solution. The pH of the reaction was maintained at 8 or above by adding 1M NaOH. The reaction was stirred for 14 hours at room temperature with nitrogen bubbling through the solution. A white slurry was formed and was washed twice using 50 mL of ethyl acetate. The resulting solid was removed using vacuum filtration. The obtained aqueous solution was acidified to a pH of 2 using 6M HCl. The aqueous solution was washed with 50 mL of ethyl acetate (3x). The ethyl acetate was dried over $MgSO_4$. The $MgSO_4$ was removed and the solution was concentrated to approximately 25 mL using a rotary evaporator. The concentrated solution was added drop-wise to 250 mL of vigorously stirring hexane, where a brown precipitate was formed. The product was dried overnight under vacuum. The molecular structure was confirmed using proton and carbon NMR (Chung, 2011).

APE-PETMP thiol-ene networks containing 0, 10, 25, and 50 mol% of DAm were synthesized from resins maintaining a 1:1 thiol:total alkene functional group stoichiometry. DAm was weighed into a scintillation vial with 1 mol% photoinitiator

(DMPA) and dissolved completely using the least amount of N,N-dimethylformamide (DMF) necessary. For Example, resins containing 50 mol% DAm require approximately 8 wt% DMF to achieve homogenous mixtures. Once completely dissolved, the appropriate amounts of PETMP and APE monomers were added to the scintillation vial and mixed thoroughly. The monomer mixture was transferred into various molds (e.g. DMA bars and MTS-Tensile dog bones) and cured for 30 minutes under a medium pressure mercury UV lamp at an intensity of 16 mW/cm^2. The samples were soaked in deionized water for 12-14 hours to remove residual DMF and were subsequently dried in a vacuum oven at 100 ^oC overnight or until a constant weight was achieved.

1.3 *Film Preparation*

Monomer resins, prepared as previously stated, were drawn down to a thickness of 2 Mils onto aluminum Q-panels (A-36 with a smooth mill finish) and steel Q-panels (QD-36 with a smooth finish). Aluminum substrates were used as received. Steel substrates were washed with acetone and wiped in a downward direction in order to remove any residual oils from the manufacture process. The glass substrates were cleaned using acetone and ethanol, and were then exposed to ozone in a UVO chamber to further remove organic impurities. White, polished venation marble was obtained from Lowe's Home Improvement. The marble was cleaned with water, ethanol, and dried under vacuum at 90 ^oC for 48 hours. The samples were subsequently cured using a UV Fusion Light Hammer 6 (10 passes at 13 ft/min) with a D bulb (685 mJ/cm^2). After curing, the samples were dried in a vacuum oven at 50 ^oC for 12-14 hours to remove residual DMF from the films.

1.4 *Characterizations*

A Varian Mercury Plus 200MHz NMR spectrometer operating at a frequency of 200.13 MHz with VNMR 6.1C software was used for the structure analysis of acrylic anhydride, phenethyl acrylamide, and dopamine acrylamide (DAm). Kinetic data was obtained using real time FTIR (RT-FTIR) spectroscopy by determining the conversions of the thiol and alkene group functionalities. The RT-FTIR studies were conducted using a Nicolet 8700 spectrometer with a KBr beam splitter and a MCT/A detector with a 320-500 nm filtered ultraviolet light source. Each sample was sandwiched between two NaCl plates (25 mm x 4 mm) and exposed to UV light with an intensity of approximately 20 mW/cm^2. A series of scans were recorded, where spectra were taken approximately 3 scans/s with a resolution of 4 cm^{-1}. Photo-DSC of the samples was obtained using a Perkin Elmer DSC 7 modified to measure heat flow of photoinitiated polymerizations. Samples were weighed into an aluminum DSC pan and placed into the sample holder without a lid, where the samples were held isothermally at 20 ^oC under a 20 mL/min flow of nitrogen. The samples were subsequently irradiated with UV light with an approximate intensity of 20 mW/cm^2. Dynamic mechanical analysis (DMA) was performed using a TA Instruments Q800 dynamic mechanical analyzer in tension film mode equipped with a gas cooling accessory. Samples were clamped at a torque of 2 in-lb. and the strain applied was 0.05%. Samples were heated from -30 ^oC to 100 ^oC at a ramp rate of 2 ^oC/min. Mechanical testing was performed using a MTS Insight^{TM} material testing machine equipped with a 10 kN load cell and preset to collect 10 data points per second. Dog bone shaped tensile samples with cross-sectional dimensions of 2.98 mm ± 0.07 mm and 1.39 mm ± 0.12 mm (thickness and width) were carefully

centered in clamps and deformed in tensile mode at a strain rate of 0.2 in/min. Young's modulus was determined from the initial linear elastic region of the stress-strain curve. Strain at break was determined concurrently during the tensile tests. Thermogravimetric analysis (TGA) was performed using a TA instruments Q50 thermogravimetric analyzer with a ceramic pan. Samples were held isothermally at 30 ^{o}C for five minutes and heated at 10 ^{o}C/min from 30 ^{o}C to 800 ^{o}C. Pull-Test adhesion data was obtained using a PosiTest AT-M Adhesion Tester (DeFelsko Corp.) according to ASTM D-4541, where LOCTITE 2h marine epoxy adhesive was used to adhere aluminum dollies (diameter of 20 mm) to the surface of the film. Cross-hatch adhesion was measured using a Cross-Cut Kit by Precision Gauge and Tool Company according to ASTM D-3359.

CHAPTER IV:

RESULTS

Polymerization kinetics for both the neat and modified APE-PETMP systems was studied using Real Time-Fourier Transform Infrared (RT-FTIR) Spectroscopy and Photo-Dynamic Scanning Calorimetry (Photo-DSC). FTIR was used to characterize the materials prior to and following UV exposure from a fiber-optic UV light source. In Figure 4 below the dashed line at 930 cm^{-1} marks the peak that corresponds to the alkene functionality. The dotted line at 2570 cm^{-1} is the peak corresponding to the thiol functionality. Additionally, FTIR was used to monitor the formation of amide linkages within the network.

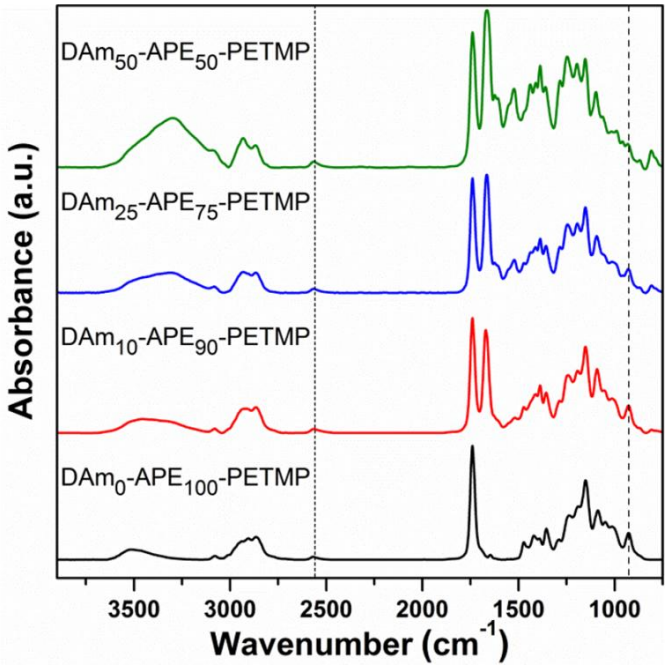

Figure 4. RT-FTIR spectra of DAm-APE-PETMP samples with varying mol% DAm.

Secondary interactions in the form of peak shifts were also observed in the RT-FTIR spectrum. As the concentration of DAm increases, peaks corresponding to amide and hydroxyl groups shift to lower wavenumbers giving evidence of an increase in hydrogen bonding. Hydrogen bonding shifts occur at the Amide I, the –OH band, and Amide II Overtone. The Amide I shifts from 1672 cm^{-1} to 1662 cm^{-1}, the –OH band shifts from 3332 cm^{-1}, and the Amide II Overtone peak is present around 3080 cm^{-1}. Figure 5 below shows the –OH band labeled with a dotted line and the Amide I peak with a dashed line.

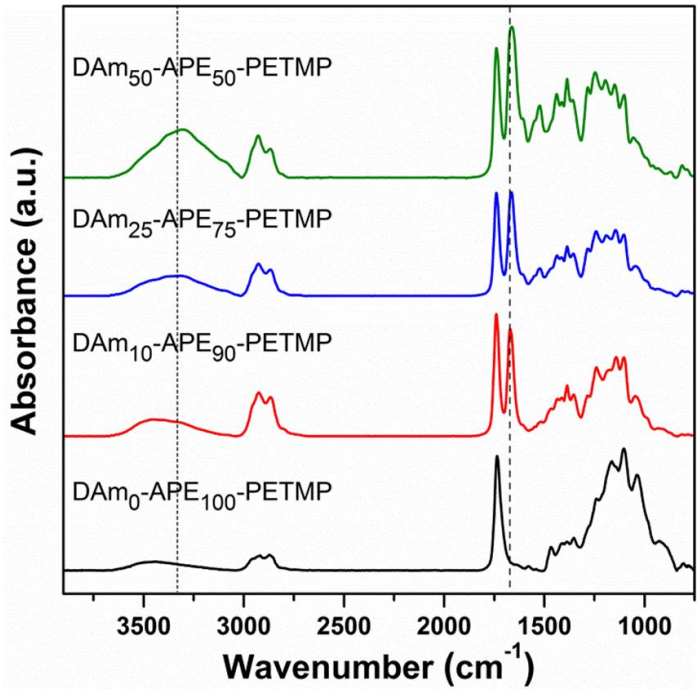

Figure 5. RT-FTIR spectra of DAm-APE-PETMP samples emphasizing secondary interactions.

Functional group conversions were determined by calculating the change in peak area with time and are shown in Figure 6. Stoichiometric consumption of thiol and

alkene functionalities was observed over all concentrations. Nearly quantitative conversions (>99%) are reached in the neat APE-PETMP system, while a slight decrease in conversion (98%) is observed with the incorporation of 10 mol% DAm. Further decreases in conversion were observed with higher concentrations, 25 and 50 mol% of Dam (93% and 82% respectively) due to a retarding or inhibiting effect caused by the catechol moiety.

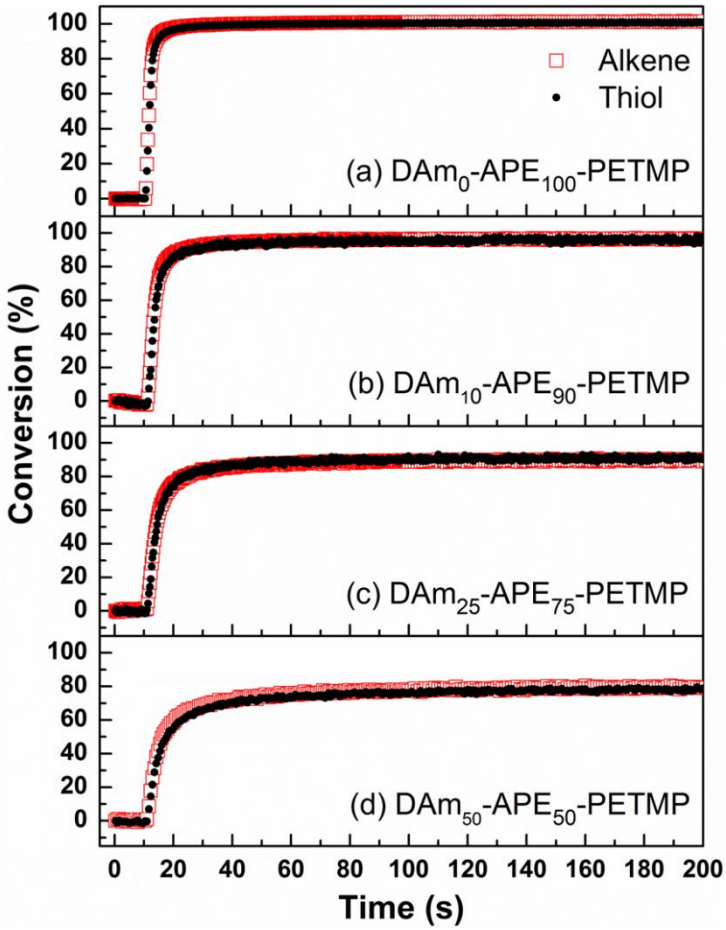

Figure 6. Kinetic plots of conversions vs. time for the DAm-APE-PETMP polymer networks with different loading percentages of DAm: a) 0 mol % DAm, b) 10 mol % DAm, c) 25 mol % DAm, and d) 50 mol % DAm. (● = thiol functionality □ = ene functionality).

Photo-DSC was used to monitor the reaction exotherm (change in enthalpy, ΔH) as the photopolymerization took place, shown in the DSC curve in Figure 7. A decrease in the peak exotherm maximum (ΔH_{MAX}) was observed with increasing concentration of DAm. ΔH_{MAX} value decreased from 258 J/g for 0 mol% DAm to 176 J/g for 50 mol% DAm. These findings complement the RT-FTIR data where the decrease in the heat of reaction can be attributed to the reduction in functional group conversion.

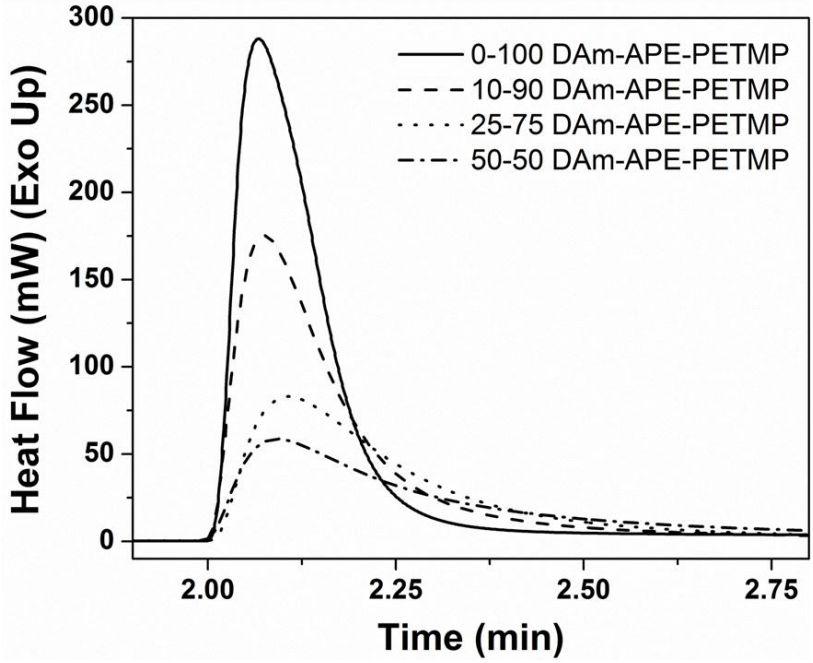

Figure 7. Photo-DSC plots of heat flow vs. time of the DAm-APE-PETMP polymer networks with varying concentrations of DAm (0-50 mol %).

Thermomechanical properties of both DAm modified networks and PhEAm modified networks were studied using Dynamic Mechanical Analysis (DMA) in order to further investigate the importance of the catechol functionality on the network properties.

Using DMA it was possible to examine both Storage Modulus of the networks and the glass transition temperature, T_g. In Figure 8, plot (a) shows an increase in Storage modulus below T_g while the rubbery storage modulus (above T_g) shows a decrease as DAm concentration increases. These changes in moduli indicate a decrease in crosslink density of the network. Plot (b) in Figure 8 shows the tan δ values vs. temperature, where an increase in T_g is observed as the DAm concentration increases which can be attributed to hydrogen bonding between catechol moieties and various proton acceptors (i.e. ethers, amides, esters, etc.). Evidence for this hydrogen bonding is shown by shifts in the amide and hydroxyl peaks in the FTIR spectra of the cured materials.

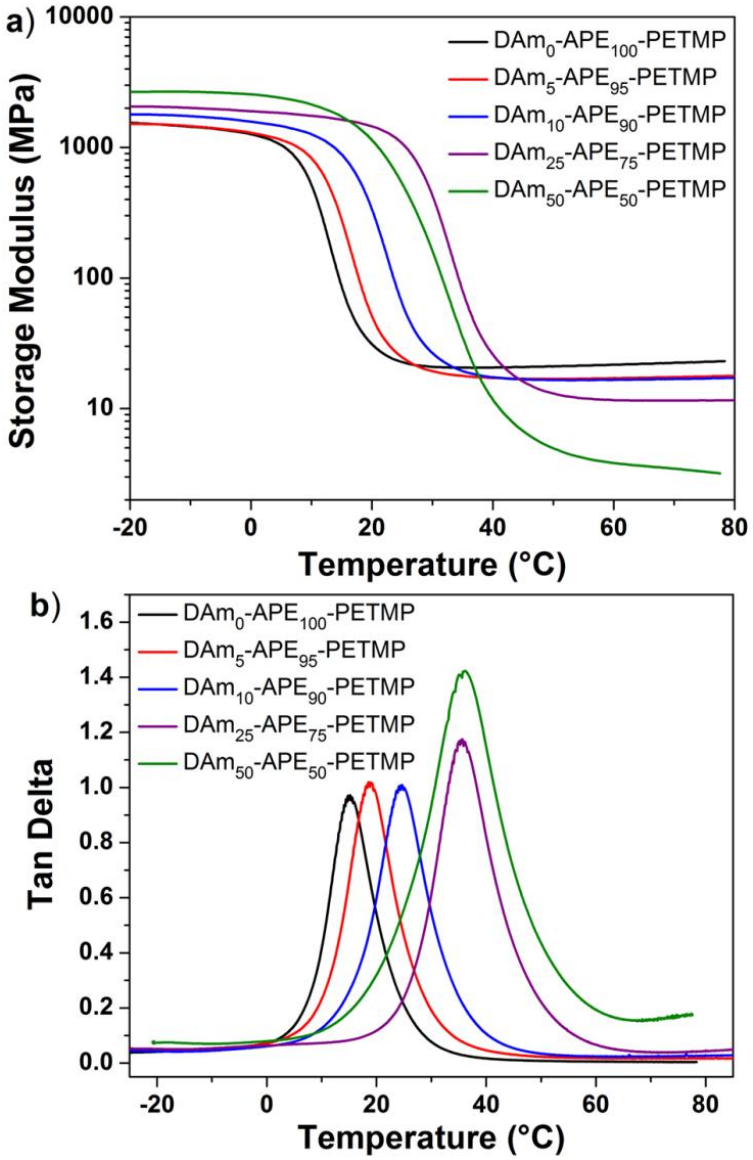

Figure 8. Plots of a) storage modulus vs. temperature and b) tan δ vs. temperature of the DAm-APE-PETMP polymer networks with varying concentrations of DAm (0-50 mol %).

The same experiment used to obtain the data above was performed on networks incorporating a monomer structurally similar to DAm, PhEAm, without the hydroxyl

functionalities. Plot (a) in Figure 9 displays the storage modulus curves for increasing concentrations of PhEAm. A decrease in rubbery storage modulus, similar to that seen with DAm, was observed with increasing PhEAm content. Unlike DAm, the decrease in crosslink density resulted in a decrease in T_g, shown in plot (b) in Figure 9 due to the lack of secondary interactions that would reinforce the network and increase the T_g as seen in the DAm-APE-PETMP networks.

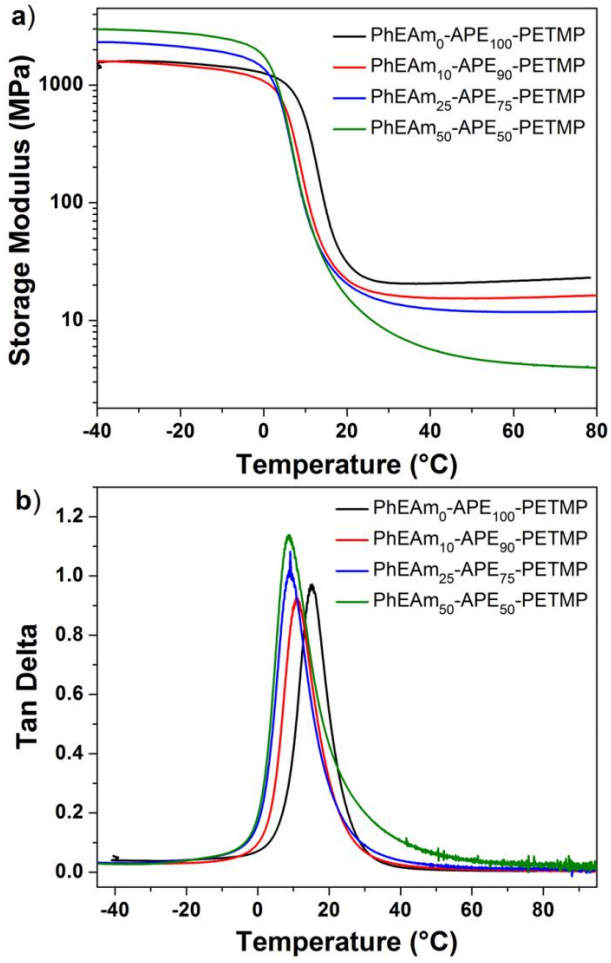

Figure 9. Plots of a) storage modulus vs. temperature and b) tan δ vs. temperature of the DAm-PhEAm-PETMP polymer networks with varying concentrations of PhEAm (0-50 mol %).

The thermomechanical properties of both DAm and PhEAm modified networks are summarized below in Table 1.

Table 1. Summary of thermomechanical properties for DAm and PhEAm modified networks.

DAm-APE-PETM (ene ratio)	Conv. (%)	T_g (°C)	fwhm (°C)[a]	E´Rub, T_g+40 (MPa)	ρ_x ($\times 10^{-3}$ mol cm^{-3})[b]
0:100	>99	15.6	9.7	20.4	2.49
10:90	98	24.6	11.4	16.7	1.98
25:75	92	35.7	12.8	11.6	1.33
50:50	83	36.1	17.5	3.30	0.379
PhEAm-APE-PETMP (ene ratio)					
0:100	>99	15.6	9.7	20.4	2.49
10:90	>99	11.1	10.9	15.4	1.90
25:75	98	9.1	11.6	12.0	1.49
50:50	93	8.9	13.5	4.83	0.601

[a]fwhm obtained from the tan δ curves; [b]crosslink density (ρ_x);

The mechanical properties of the DAm modified networks were tested to determine Young's modulus and are displayed in Figure 10. A drastic increase was observed with 10 mol% DAm, followed by a gradual decrease back to a value equal to that of the pristine material. Lowered crosslink density dominates the contributions to mechanical behavior which is shown by the modulus values. An increase in toughness of the materials is observed due to the polymer chain's ability to rearrange upon deformation due to a decrease in crosslink density.

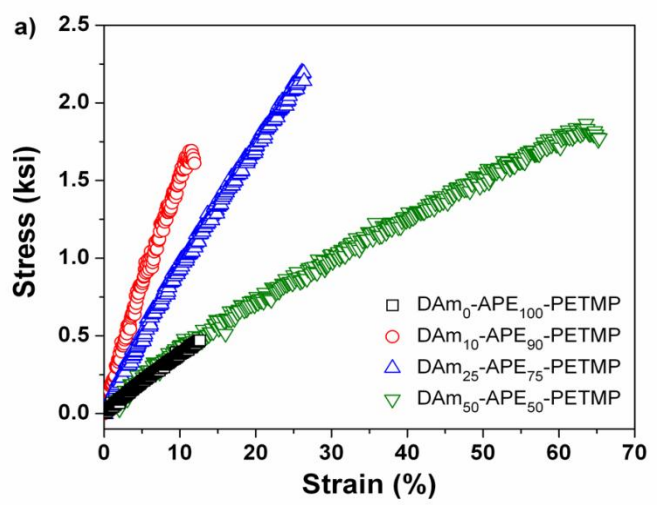

Figure 10. Mechanical testing data: a) stress vs. strain plots of the DAm-APE-PETMP polymer networks with varying concentrations of DAm: neat APE-PETMP (□), 10 mol % DAm (○), 25 mol % DAm (△), and 50 mol % DAm (▽) and b) modulus (■) and strain at break (○) as a function of dopamine acrylamide loading percentage.

Macroscopic adhesion of the DAm-APE-PETMP materials to various substrates (glass, steel, and aluminum) was investigated using a pull-off test and cross-hatch adhesion. Films were drawn down at a thickness of 2 Mils (50 μm) and cured. An increase in adhesion properties was observed on all substrates as the concentration of DAm increased possibly due to favorable interactions between the substrates and the DAm-APE-PETMP material. In Figure 11 the increase in adhesion is shown by the pull-off force required at different mol% concentrations of DAm. Figure 12 is a photograph taken to show examples of the substrates for both cross-hatch adhesion and pull-off adhesion tests after testing was completed to demonstrate how the different types of failure looked. Shown in part (a) of Figure 12 are results of the cross-hatch adhesion test,

which show progressively less of the network being removed with higher concentrations of DAm in the network. In part (b) are results of the pull-off adhesion test which show an adhesive type failure where the network is removed from the substrate for 0% and 10% DAm loading while there was a multimodal failure for 25% and 50% DAm loading where the samples failed both adhesively and cohesively (shown by the grey epoxy material remaining partially on the substrate. Table 2 shows adhesion values across all of the tested concentrations, substrates, and both pull-off and cross-hatch adhesion testing methods. Table 2 also includes adhesion values for a marble substrate, however, the stone substrate failed before the epoxy adhesive/thiol-ene network interface failed which meant that little to no viable data was obtained from these tests other than to say that the adhesion of the network to the stone was higher than the forces holding the stone together.

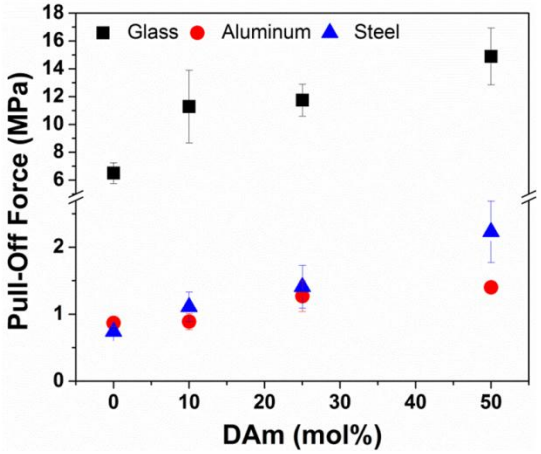

Figure 11. Adhesion strength of the DAm-APE-PETMP films as function of DAm content.(■) Glass; (●) Aluminum; (▲) Steel

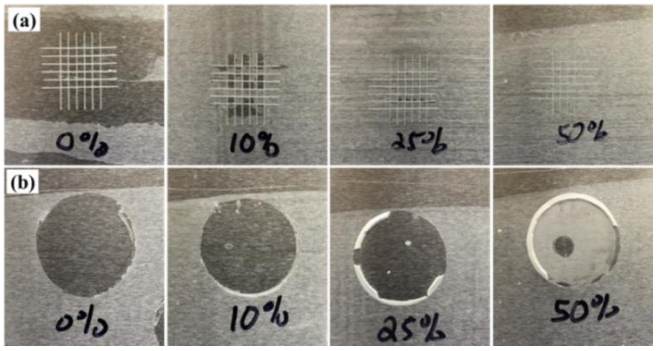

Figure 12. Photos of the (a) cross-hatch and (b) pull-off adhesion tests of DAm-APE-PETMP films on aluminum substrates.

Table 2. Summary of adhesion values for DAm-APE-PETMP across all substrates.

	Pull-Off Adhesion (MPa)				Cross-hatch Adhesion			
DAm-APE-PETMP (ene ratio)	Glass	Al	Steel	Marble	Glass	Al	Steel	Marble
0:100	6.51±0.74	0.87±0.05	0.74±0.05	2.65±0.39[a]	0B	0B	0B	0B
10:90	11.29±2.61	0.89±0.12	1.11±0.22	2.41±0.28[a]	1B	1B	0B	2B
25:75	11.75±1.15[a]	1.27±0.23	1.41±0.32	3.32±0.22[a]	4B	3B	5B	4B
50:50	14.89±2.04[a]	1.40±0.09[b]	2.23±0.46[b]	2.26±0.34[a]	4B	4B	5B	4B

[a]Substrate failed during pull-test while the adhesive bond remained intact. [b]Mixed mode failure (partial adhesive/cohesive)

CHAPTER V:

CONCLUSIONS

While the main research goal of this project was the investigation of adhesion in a thiol-ene polymer network modified with a catechol functional monomer, various other interesting changes in thermomechanical and mechanical properties were observed. First, bioinspired thiol-ene polymer networks via photopolymerization of a ternary monomer resin including dopamine acrylamide were synthesized successfully. Next, during this synthesis, overall conversion values decreased slightly as the concentration of DAm increased; however, a 1:1 stoichiometry was maintained between thiol and alkene functionalities. An increase in T_g was observed with increasing concentration of DAm due to an increase in hydrogen bonding within the networks, shown in an FTIR study, indicated by shifts of the amide and hydroxyl peaks to lower wavenumbers. In addition, similar trends were observed in the tensile properties of the materials, reflecting the interplay between the hydrogen bonding and crosslink density. Finally, improved macroscopic adhesion of DAm-APE-PETMP coatings to a range of substrates was shown by systematically varying the amount of DAm in the network.

REFERENCES

1. Winkler, E. M., *Stone In Architecture*. Third ed.; Springer-Verlag: Berlin, 1994.

2. Amoroso, G. G.; Fassina, V., *Stone Decay and Conservation*. Elsevier: Amsterdam, 1983; Vol. 11.

3. Charola, E. E. *Review of the Literature on the Topic of Acidic Deposition on Stone*; National Center for Preservation Technology and Training: Natchitoches, Louisiana, 1998.

4. Price, C. A., *Stone Conservation: Overview of Current Research*. Getty Conservation Institute: Los Angeles, 1996.

5. Nason, C.; Roper, T.; Hoyle, C.; Pojman, J. A., *Macromolecules* 2005, *38* (13), 5506-5512.

6. Hoyle, C. H.; Bowman, C., *Angew. Chem. int. Ed.* 2010, *49* (9), 1540-1573.

7. O'Brien, A.; Cramer, N.; Bowman, C., *J. Polym. Sci. A. Polym. Chem.* 2006, *44* (6), 2007-2014.

8. Hammaker, J. R.; Mash, E. A., *J. Macromol. Sci. A* 2008, 45, 865-871

9. Frost, C. G.; Penrose, S. D.; Gleave, R., *Organic & Biomolecular Chemistry* 2008, 6, 4340-4347

10. Chung, H.; Glass, P.; Pothen, J. M.; Sitti, M.; Washburn, N. R., *Biomacromolecules* 2011, 12, 342-347.

11. Stewart, R. J.; Weaver, J. C.; Morse, D. E.; Waite, J. H., *J. Exp. Biol.* 2004, 207, 4727-4734.